PROCEEDINGS OF SCIENCE

Final measurement of the Muon Anomalous Magnetic Moment at Fermilab

Paolo Girotti[a,b,†,*]

[a] *INFN, Sezione di Pisa, Pisa, Italy*

[b] *INFN, Laboratori Nazionali di Frascati, Frascati, Italy*

E-mail: paolo.girotti@lnf.infn.it

The Muon $g-2$ Experiment at Fermilab has published the final measurement of the positive muon anomalous magnetic moment, which combines three measurements across six years of data collection. The measured value of $a_\mu = 1\,165\,920\,705(148) \times 10^{-12}$ achieves a total precision of 127 parts per billion (ppb), representing more than a fourfold improvement over the previous Brookhaven National Laboratory (BNL) E821 measurement. This result is the most precise determination of the muon magnetic anomaly to date and provides a critical benchmark for testing the Standard Model at the highest precision. This report discusses the hardware upgrades and the analysis improvements of the final Run-4/5/6 measurement with respect to the previous ones.

The 26th international symposium on spin physics (SPIN2025)
21–26 September, 2025
Qingdao (Tsingtao), Shandong Province, China

[†] on behalf of the Muon $g-2$ collaboration.
[*] Speaker

PoS(SPIN2025)018

1. Introduction

The anomalous magnetic moment of the muon a_μ = (g-2)/2 is a measurable quantity that represents a precision test for the Standard Model (SM). Its value encodes the sum of all virtual quantum interactions between the muon and the magnetic field. The SM prediction includes contributions from Quantum Electrodynamics (QED), Electroweak (EW), and Hadronic sectors (Hadronic Vacuum Polarization, HVP; and Hadronic Light-by-Light, HLbL). Any discrepancy between the measured and predicted values represents a signal of new physics due to unaccounted virtual interactions. The muon is more sensitive to Beyond Standard Model (BSM) physics with respect to the electron: its mass, approximately 200 times that of the electron, yields an enhancement factor of $(m_\mu/m_e)^2 \approx 4 \times 10^4$ in sensitivity to heavy virtual states.

Multiple experiments measured the anomalous magnetic moment of the muon with increasing precision since the 1960s. The E821 Experiment at BNL measured a_μ with 0.54 ppm precision in 2006 [1] and the measured value was in tension with the theory prediction to a 3.7σ level [2]. The BNL storage ring was then moved to Fermilab in 2013 to repeat the measurement with higher statistics and improved detectors. The first [3] and second [4] measurements at Fermilab confirmed the BNL measurement with improved accuracies of 460 ppb and 210 ppb respectively and increased the overall tension with the theory to 5.2 σ. The theoretical landscape, however, has since evolved: increasingly precise ab-initio Lattice-QCD determinations of the hadronic vacuum polarization contribution were in tension with the dispersive calculations based on $e^+e^- \rightarrow hadrons$ data [5, 6]. Moreover, a new measurement of $e^+e^- \rightarrow \pi^+\pi^-$ cross sections by the CMD-3 experiment [7] strongly disagreed with previous experiments. For these reasons, the latest theory paper [8] excluded the dispersive-only predictions in the determination of the SM a_μ value of $a_\mu^{SM} = 1\,165\,920\,330(620) \times 10^{-12}$ (530 ppb).

This article discusses the latest a_μ measurement of the Muon $g-2$ Experiment at Fermilab, based on the final Run-4/5/6 datasets collected between 2021 and 2023 [9]. Figure 1 compares the statistics of this measurement with the previous datasets. Comprehensive details of the experimental design and analysis techniques are covered in the Fermilab Muon $g-2$ Collaboration's previous publications [10–13]. This contribution will focus on the most relevant details and improvements of the latest analysis with respect to the previous results.

2. The Muon $g-2$ Experiment at Fermilab

The Fermilab Experiment measures the muon decays coming from a beam of 3.1 GeV/c polarized muons. The muon beam is extracted from the collision products of a 8 GeV proton beam onto a fixed target. The ultra pure beam enters a magnetic storage ring with a diameter of 14 m and a homogeneous vertical magnetic field of 1.45 T. The muon decays are measured for 700 μs in each beam injection, with an average injection rate of 11 Hz. The magnetic field provides weak radial focusing and defines the axis of muon spin precession. The muon decay produces positrons that, having a smaller momentum, curl inward until they hit a calorimeter station. High energy positrons in the muon's rest frame are emitted preferably in the direction of the muon spin. In

PoS(SPIN2025)018

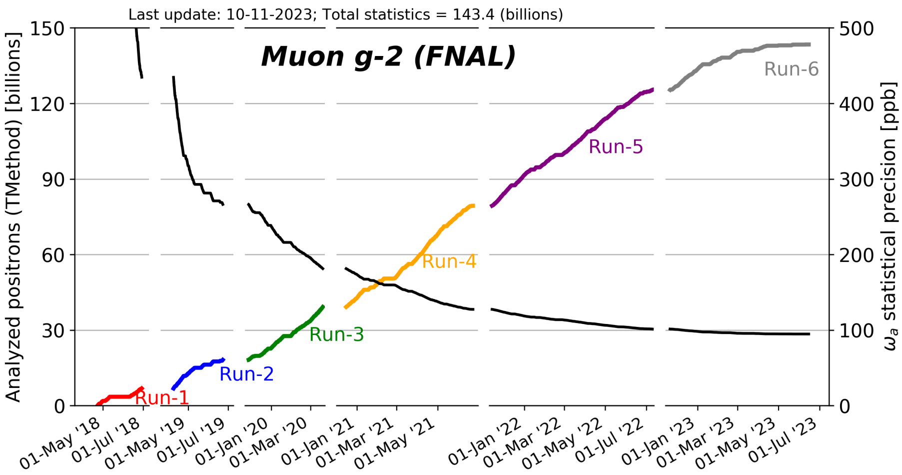

Figure 1: Cumulative statistics (left axis) of the six datasets of the Fermilab Experiment and the respective statistical uncertainty of ω_a (right axis). The number of positrons are selected in energy and time according to: E > 1700 MeV, t > 30 μs (TMethod selection).

the laboratory frame, this translates to different observed positron energy spectra depending on the orientation of the muon spin with respect to the boost vector. This results in a varying number of detected positrons above a certain threshold across time. This modulation occurs at the anomalous precession frequency ω_a and is proportional to the anomalous magnetic moment:

$$\vec{\omega}_a = \vec{\omega}_s - \vec{\omega}_c = -\left(\frac{g-2}{2}\right)\frac{e\vec{B}}{m_\mu} \equiv -a_\mu \frac{e\vec{B}}{m_\mu}, \tag{1}$$

where ω_s is the spin precession frequency, ω_c is the cyclotron frequency, and B is the magnetic field. e and m_μ are the electric charge and the mass of the muon.

There are 24 electromagnetic calorimeters equally spaced along the inner side of the magnetic ring, each one consisting of 54 PbF_2 crystals arranged in a 9×6 matrix [14]. Each crystal is coupled with a SiPM to collect the Cherenkov light emitted by the EM shower. Two straw-tube tracker stations placed in front of two calorimeters measure the positron trajectory before they collide with the crystals [15]. A state-of-the-art laser-based system is used to synchronize the detectors in time and correct for gain fluctuations [16].

The extraction of a_μ relies on three measurements: the muon anomalous precession frequency ω_a, the magnetic field strength B in terms of the Larmor precession frequency of the proton ω_p [17], and the muon distribution in the storage ring M. The full expression for a_μ is:

$$a_\mu = \frac{\omega_a}{\tilde{\omega}'_p}\frac{g_e}{2}\frac{m_\mu}{m_e}\frac{\mu'_p}{\mu_e}, \tag{2}$$

where the first fraction contains the quantities measured by the Muon $g-2$ Experiment and the other terms come from precise external measurements. In particular,

$$\frac{\omega_a}{\tilde{\omega}'_p} \equiv R'_\mu = \frac{f_{clock}\,\omega_a^m(1 + C_e + C_p + C_{pa} + C_{dd} + C_{ml})}{f_{calib}\langle\omega_p(x,y,\phi) \times M(x,y,\phi)\rangle(1 + B_k + B_q)}, \tag{3}$$

where f_{clock} is the blinded hardware frequency and f_{calib} represents the absolute field calibration. C_e, C_p, C_{pa}, C_{dd}, and C_{ml} are corrections related to the dynamics of the muon beam. C_e is the largest correction, with a value of 347 ppb and an uncertainty of 27 ppb, and is associated with the momentum spread of the muon beam. B_k and B_q are magnetic field corrections due to fast transient magnetic fields generated by the kicker and quadrupole systems.

3. Run-4/5/6 upgrades

Several hardware interventions were performed to the apparatus before and during the Run-4/5/6 data taking periods to either improve the system or enable new and more precise systematic studies. This section will summarize the most relevant ones.

Toward the end of Run-3, the kicker's voltages were increased to the nominal 165 kV, ensuring better centering of the beam in the storage region [19]. This greatly reduced the magnitude of C_e.

One of the most significant advancements was the implementation of a Radio Frequency (RF) damping system introduced before Run-5 [18]. By applying a resonant pulse to the electrostatic quadrupole system within the first 10 μs of injection, Coherent Betatron Oscillations (CBO) were reduced by almost an order of magnitude. Figure 2 illustrates the RF pulsing scheme.

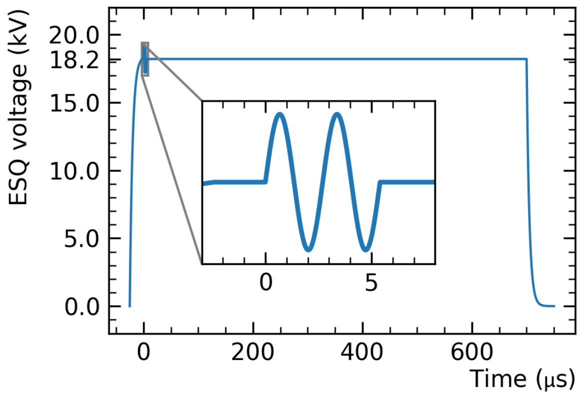

Figure 2: Pulsing scheme of the electrostatic quadrupoles (ESQ) during the 700 μs window of a stored muon bunch. The inset zooms on the quick pulsing pattern introduced by the new RF system.

A new Minimally Intrusive Scintillating Fiber detector (MiniSciFi) was built to directly measure the muon beam distribution in the storage region. The device can be inserted for the dedicated measurement or stowed away during normal physics runs. The device consists of three vertical or horizontal scintillating fibers that can be translated to line-scan the entire transversal plane. Figure 3 shows the detector inserted in the vertical fibers configuration. The measurements conducted with this device helped to cross check the muon beam distribution extrapolations obtained with the calorimeters and tracker stations. In addition, it precisely determined the momentum distribution and the correlation between momentum and relative time in the muon bunch. These measurements, together with more robust analysis methods reduced the uncertainty of C_e, the leading correction to ω_a^m of Equation 3, from 32 ppb in Run-2/3 to 27 ppb.

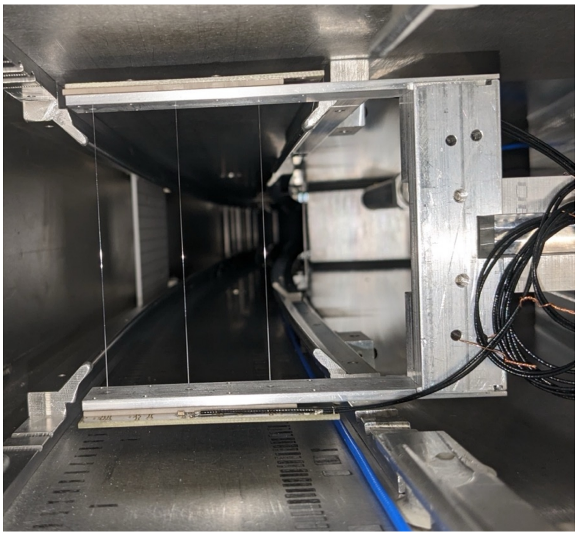

Figure 3: The MiniSciFi detector with vertical fibers inserted in the muon storage region.

A new independent free-space laser magnetometer was built and operated to measure the time-dependent residual magnetic fields from eddy currents induced by the fast kicker magnets [19]. The magnetometer technique is based on Faraday rotation in Terbium Gallium Garnet (TGG) crystals located between the kicker plates. The system sends a laser light through a glass window toward the crystals and then measures the laser polarization angle of the returning beam. The measurements are performed in dedicated systematic runs with no beam. The fiber-based magnetometer, which was used previously, was also upgraded to be less sensitive to mechanical vibrations. Two of the three kickers were measured at several transverse positions and the measurements obtained with the two systems agree within uncertainties. New measurements at large transverse positions (18 mm from the nominal orbit radius) revealed eddy currents higher by a factor of 2. This finding was investigated with additional measurements on a mock-up model of the kicker system, and led to a larger B_k correction and systematic uncertainty relative to Run-2/3. The Run-2/3 correction was updated accordingly for the final combination.

An unexplained slowly-varying gain-like term was observed in the Run-1 and Run-2/3 calorimeter data [10, 13]. Following the completion of the experiment, a calorimeter station was extracted from the experimental hall and a small scale replica of the laser calibration system was developed to investigate the phenomenon. High rates of incident positrons cause a gain sag in calorimeter electronics due to capacitor depletion, which recovers with a $\sim 6\ \mu$s time constant. Although the magnitude of this sag is below the initial 10^{-4} design specification, it oscillates at the ω_a frequency with a phase shift and contributes to a greater sensitivity than previously estimated. A new correction for this effect was measured and applied to all datasets. The slow-term related systematic uncertainty increased to 11-22 ppb depending on the dataset, but the nature of the effect is now fully understood.

4. Systematic uncertainties

Table 1 lists the measured quantities of Equation 3 and the associated systematic uncertainty, comparing the Run-4/5/6 results to the previous measurements. The total uncertainty on a_μ is 139 ppb, consisting of 114 ppb of statistical uncertainty and 76 ppb of systematic uncertainty. For Run-4/5/6, there is no dominant source of systematic uncertainties, so improving one uncertainty would not improve the overall result by much. All uncertainties have reached or surpassed their design target.

Quantity	Description	Run-1 (ppb)	Run-2/3 (ppb)	Runs 4/5/6 (ppb)
ω_a^m	(statistical unc.)	434	201	114
ω_a^m	(systematic unc.)	56	25	30
$\langle \omega'_p \times M \rangle$	(syst. unc.)	56	46	48
C_e	Electric Field	489 ± 53	451 ± 32	347 ± 27
C_p	Pitch Correction	180 ± 13	170 ± 10	175 ± 9
C_{pa}	Phase-Acceptance	-158 ± 75	-27 ± 13	-33 ± 15
C_{dd}	Differential Decay	-	-15 ± 17	26 ± 27
C_{ml}	Muon Loss	-11 ± 5	0 ± 3	0 ± 2
B_k	Kicker Transient	-27 ± 37	-21 ± 13	-37 ± 22
B_q	ESQ Transient	-17 ± 92	-21 ± 20	-21 ± 20
R'_μ	Systematic unc.	157	70	76
a_μ	Total unc.	462	215	139

Table 1: Evolution of corrections and uncertainties for the Fermilab Muon $g-2$ Experiment. Numbers reproduced from [3, 4, 9].

5. Results and conclusions

In June 2025, the Muon $g-2$ Collaboration released the final measurement of the muon anomalous magnetic moment relative to the Run-4/5/6 datasets, with a precision of 139 ppb. The superior statistical power of this larger dataset, along with additional dedicated measurements, enabled further cross-checks of the Run-1 and Run-2/3 results. Three small corrections with corresponding uncertainty adjustments were identified and applied when combining the Run-4/5/6 measurement with the Run-1 and Run-2/3 ones. These corrections shifted the Run-1 and Run-2/3 results by 50 ppb and 98 ppb, respectively, and result in a total systematic uncertainty of 78 ppb for the adjusted Run-2/3 result. Further description of these corrections can be found in [9]. The combined FNAL average, Run-1-6, with a total uncertainty of 127 ppb, assumes fully correlated systematic uncertainties between the results. The final measured values for the Fermilab Muon $g-2$ Experiment are:

$$a_\mu^{Exp}(\text{FNAL, Run-4/5/6)}) = 1\,165\,920\,710(162) \times 10^{-12} \text{ (139 ppb)}\,, \tag{4}$$

$$a_\mu^{Exp}(\text{FNAL, Run-1-6}) = 1\,165\,920\,705(148) \times 10^{-12} \text{ (127 ppb)}\,. \tag{5}$$

When combined with the BNL result, the new experimental world average is:

$$a_\mu^{Exp}(\text{World, 2025}) = 1\,165\,920\,715(145) \times 10^{-12}\ (124\ \text{ppb})\,. \tag{6}$$

Figure 4 compares the measurements from individual datasets and the combined ones.

The theoretical landscape in 2025 is still defined by the discrepancies between different e^+e^- cross-section data from different experiments and the tension with the results obtained with Lattice-QCD, as described in Section 1. The latest consensus on the theoretical prediction is defined in [8] and relies exclusively on Lattice-QCD calculations. The current theoretical prediction:

$$a_\mu^{Th}(\text{WP2025}) = 1\,165\,920\,330(620) \times 10^{-12}\ (530\ \text{ppb}) \tag{7}$$

aligns more closely with the experimental value, agreeing at the 0.6 σ level. Regardless of how will the theoretical framework evolve in the coming years, the final Muon $g-2$ result surpassed the original design goals and will provide a long standing benchmark for all SM comparisons.

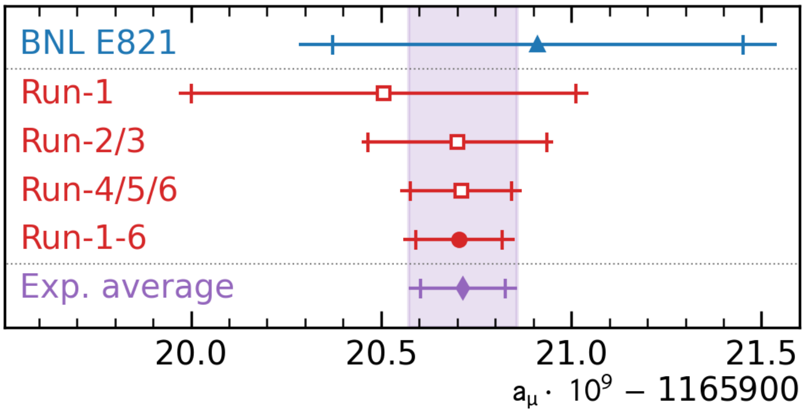

Figure 4: Measured values of a_μ from BNL and FNAL and the combined experimental average. The inner tick marks indicate the statistical contribution to the total uncertainties. Figure from [9].

Acknowledgements

The Muon $g-2$ Experiment was performed at the Fermi National Accelerator Laboratory, a U.S. Department of Energy, Office of Science, HEP User Facility. Fermilab is managed by Fermi Forward Discovery Group, LLC, acting under Contract No. 89243024CSC000002. Additional support for the experiment was provided by the Department of Energy offices of HEP, NP, and ASCR (USA), the National Science Foundation (USA), the Istituto Nazionale di Fisica Nucleare (Italy), the Science and Technology Facilities Council (UK), the Royal Society (UK), the National Natural Science Foundation of China (Grant No. 12211540001, 12075151), MSIP, NRF and IBS-R017-D1 (Republic of Korea), the German Research Foundation (DFG) through the Cluster of Excellence PRISMA+ (EXC 2118/1, Project ID 39083149), the European Union Horizon 2020 research and innovation programme under the Marie Skłodowska-Curie grant agreements No. 101006726, No. 734303, and European Union STRONG 2020 project under grant agreement No. 824093 and the Leverhulme Trust, LIP-2021-01.

References

[1] G. W. Bennett et al. (Muon $g-2$ Collaboration), *Final report of the E821 muon anomalous magnetic moment measurement at BNL*, Phys. Rev. D **73**, 072003 (2006)

[2] T. Aoyama et al., *The anomalous magnetic moment of the muon in the Standard Model*, Phys. Rep. **887** (2020)

[3] B. Abi et al. (Muon $g-2$ Collaboration), *Measurement of the Positive Muon Anomalous Magnetic Moment to 0.46 ppm*, Phys. Rev. Lett. **126**, 141801 (2021)

[4] D. P. Aguillard et al. (Muon $g-2$ Collaboration), *Measurement of the Positive Muon Anomalous Magnetic Moment to 0.20 ppm*, Phys. Rev. Lett. **131**, 161802 (2023)

[5] Sz. Borsanyi et al., *Leading hadronic contribution to the muon magnetic moment from lattice QCD*, Nature **593**, pages 51–55 (2021)

[6] C. Alexandrou et al., *Lattice calculation of the short and intermediate time-distance hadronic vacuum polarization contributions to the muon magnetic moment using twisted-mass fermions*, Phys. Rev. D **107**, 074506 (2023)

[7] F. V. Ignatov et al. (CMD-3 Collaboration), *Measurement of the pion form factor with CMD-3 detector and its implication to the hadronic contribution to Muon (g-2)*, Phys. Rev. Lett. **132**, 231903 (2024)

[8] R. Aliberti et al., *The anomalous magnetic moment of the muon in the Standard Model: an update*, Phys. Rep. **1143** Pages 1-158 (2025)

[9] D. P. Aguillard et al. (Muon $g-2$ Collaboration), *Measurement of the Positive Muon Anomalous Magnetic Moment to 127 ppb*, Phys. Rev. Lett. **135**, 101802 (2025)

[10] T. Albahri et al. (Muon $g-2$ Collaboration), *Measurement of the anomalous precession frequency of the muon in the Fermilab Muon g-2 Experiment*, Phys. Rev. D **103**, 072002 (2021).

[11] T. Albahri et al. (Muon $g-2$ Collaboration), *Magnetic-field measurement and analysis for the Muon g-2 Experiment at Fermilab*, Phys. Rev. A **103**, 042208 (2021).

[12] T. Albahri et al. (Muon $g-2$ Collaboration), *Beam dynamics corrections to the Run-1 measurement of the muon anomalous magnetic moment at Fermilab*, Phys. Rev. Accel. Beams **24**, 044002 (2021).

[13] D. P. Aguillard et al. (Muon $g-2$ Collaboration), *Detailed report on the measurement of the positive muon anomalous magnetic moment to 0.20 ppm*, Phys. Rev. D **110**, 032009 (2024).

[14] L.P. Alonzi et al., *The calorimeter system of the new muon g-2 experiment at Fermilab*, Nucl. Instrum. Methods Phys. Res. A **824**, 718-720 (2016)

[15] B.T. King et al., *The straw tracking detector for the Fermilab Muon g-2 Experiment*, JINST **17** P02035 (2022)

[16] A. Anastasi et al., *The laser-based gain monitoring system of the calorimeters in the Muon g-2 experiment at Fermilab*, JINST **14**, P11025 (2019)

[17] E. Swanson et al., *The fixed probe storage ring magnetometer for the Muon g-2 experiment at Fermi National Accelerator Laboratory*, Nucl. Instrum. Methods Phys. Res. A **1075**, 170338 (2025)

[18] On Kim et al., *Reduction of coherent betatron oscillations in a muon g-2 storage ring experiment using RF fields*, New J. Phys. **22**, 063002 (2020)

[19] A.P. Schreckenberger et al., *The fast non-ferric kicker system for the Muon g-2 Experiment at Fermilab*, Nucl. Instrum. Meth. A **1011**, 165597 (2021)